Synthesis, Characterization, and Theoretical Study of Novel Charge-Transfer Complexes Derived from 3,4-Selenadiazobenzophenone

Haider Shanshool Mohammed and Nuha Hussain Al-Saadawy*

Department of Chemistry, College of Science, University of Thi-Qar, Muthanna, 64001, Iraq

* ***Corresponding author:***

email: Nuhaalshather@yahoo.com

Received: July 25, 2022
Accepted: September 25, 2022

DOI: 10.22146/ijc.76537

Abstract: *In the current study, a direct method was used to synthesize a new series of charge-transfer complex compounds. Reaction of different quinones with 3,4-selenadiazo benzophenone in a 1:1 mole ratio by acetonitrile gave a unique charge-transfer complex compound in a good yield. All compounds were characterized by UV-Vis, FTIR, ^{1}H-NMR, and ^{13}C-NMR. The analysis findings agreed with the produced compound's proposed chemical structures. The molecular structure of the produced charge-transfer complex compounds has been investigated using density functional theory. The basis set of 3–21G geometrical designs throughout the geometry optimization, HOMO surfaces, LUMO surfaces, and energy gap has been created. The acceptor and donor have also been studied by comparing the HOMO energies of the charge-transfer complexes. The lower case, electron affinity, ionization potential, electronegativity, and electrophilicity where the total energies of donor-acceptor system and geometric structures demonstrate this structure's stability. Additionally, the donor-acceptor system has higher reactivity than other systems and larger average polarizability when compared to the donor and acceptor. The findings of this study enable us to choose the kind of bridge that will interact with the donor and acceptor to determine the physical characteristics of the donor-bridge-acceptor.*

Keywords: *charge-transfer complexes; 3,4-selenadiazo benzophenone; acetonitrile; difference quinones*

■ INTRODUCTION

Since the nineteenth century, there have been known to be organoselenium compounds. Organoselenium chemistry developed, and a more organized understanding and reactions started to take the shape of their structures [1]. Selenadiazoles, which have one atom of selenium and two nitrogen atoms, are a significant type of heterocyclic organoselenium compounds [2]. The majority of reactions used to synthesize selenadiazole are known to be based on the reaction between SeO_2 and diamine [3-5]. 1,2,5-Selenadiazoles are widely and extensively investigated forms of selenadiazoles for a variety of applications due to their simplicity in preparation [6]. Heterocyclic compounds of organoselenium (1,2,5-selenadiazole) have drawn interest as light emitters, organic metals, drugs, medicinally important species, oil additives, and so forth. Alternately, a variety of groups have been developed for selenium, permitting, for example, electrophilic enantioselective additions variants of a number of additional selenium reaction types [7]. There has recently been a lot of interest in research on the complexes of charge-transfer for selenadiazole compounds with quinones that function as electron acceptors, such as *p*-benzoquinone, anthraquinone, tetrachlorobenzoquinone, 7,7,8,8-Tetracyano quino dimethane (TCNQ), and 1,4-Dihydroxyanthraquinon [8] that we used in our study.

The physical studies of these new complexes have been described [9-10]. Charge transfer complexes (CT complexes) have received a great deal of attention because of their special chemical and physical characteristics and the potential for their use in a variety of fields, including optical communications and optoelectronics [11-12], solar cells and organic semiconductors [13-17], pharmacology (anti-inflammatory and antibacterial activity) [18-22]. Charge-transfer complexes of selenadiazole have been synthesized and studied spectroscopically [23-28].

In this paper, we report the synthesis of new compounds of charge-transfer complexes through the reaction of 3,4-selenadiazo benzophenone with different quinones such as (*p*-benzoquinone, anthraquinone, Tetra chlorobenzoquinone, 7,7,8,8-Tetracyanoquinodimethane, and 1,4-Dihydroxyanthraquinon).

■ EXPERIMENTAL SECTION

Materials

The chemicals used included 3,4-diamino benzophenone (Sigma-Aldrich), ethanol absolute, acetonitrile (Fluka.), *p*-benzoquinone (Sigma-Aldrich), anthraquinone (Sigma-Aldrich), Tetrachlorobenzoquinone (Fluka), 7,7,8,8-Tetracyanoquinodimethane (Sigma-Aldrich), 1,4-Dihydroxyanthraquinon (Strem chemicals Inc.), selenium dioxide powder (Strem chemicals Inc.), nitric acid (HGB).

Instrumentation

^{1}H-NMR spectrum was recorded on Bruker 500 MHz spectrometers with TMS as an inner reference utilizing DMSO-d_6 as the solvent. Infrared spectra were recorded with KBr disc using an FT-IR spectrophotometer Shimadzu model 8400 S in 4000–250 cm^{-1}, UV-Visible Spectrophotometer Shimadzu double-beam model UV-1650 (Japan) equipped quartz cells with 1.00 cm, electrothermal melting point apparatus. Gaussian (G09W) was used for the DFT calculation employing the basis set of 3–21G.

Procedure

Preparation of selenadiazo-3,4-diamino benzophenone

3,4-Diamino benzophenone (4.24 g, 20 mmol) was dissolved in 30 mL of ethanol and mixed with 2.2 g (20 mmol) of selenium dioxide (SeO_2), using a round bottom flask. The mixture was refluxed in a water bath for 2 h until a coffee-colored solution was formed. After that, the solution was cooled, filtered, and washed with hot ethanol to obtain a coffee-colored precipitate with a yield of 80% and a melting point of 95 °C, as shown in Scheme 1. The Rf value is 0.73 (7:3) (Ethyl acetate:*n*-hexane).

Preparation of benzoquino-3,4-selenadiazo benzophenone (A)

3,4-Selenadiazo benzophenone (1.147 g, 4 mmol) was dissolved in 30 mL of acetonitrile and mixed with 0.432 g (4 mmol) of *p*-benzoquinone dissolved in 30 mL of acetonitrile and heated using reflux in a water bath for 3 h. The solution was cooled and evaporated by a rotary evaporator and washed with small amounts of acetonitrile to obtain a pure and shiny precipitate with a yield of 79% and a melting point of 108 °C, as shown in Scheme 2. Rf value = 0.70 (7:3) (Ethyl acetate:*n*-hexane).

Preparation of anthraquino-3,4-selenadiazo benzophenone (B)

3,4-Selenadiazo benzophenone (1.147 g, 4 mmol) was dissolved in 30 mL of acetonitrile and mixed with 0.832 g (4 mmol) of anthraquinone dissolved in 30 mL of acetonitrile and heated using reflux in a water bath for 3 h. The solution was cooled and evaporated by a rotary evaporator and washed with small amounts of acetonitrile to obtain a pure and shiny light yellow crystals precipitate formed with a yield of 90% and a melting point of = 190 °C, as shown in Scheme 2. Rf value = 0.60 (7:3) (Ethyl acetate:*n*-hexane).

Preparation of tetrachlorobenzoquino-3,4-selenadiazo benzophenone (C)

3,4-Selenadiazo benzophenone (1.147 g, 4 mmol) was dissolved in 30 mL of acetonitrile and mixed with 0.983 g (4 mmol) of tetrachlorobenzoquinone in 30 mL of acetonitrile and heated using reflux in a water bath for 3 h. The solution was cooled and evaporated by a rotary evaporator and washed with small amounts of acetonitrile

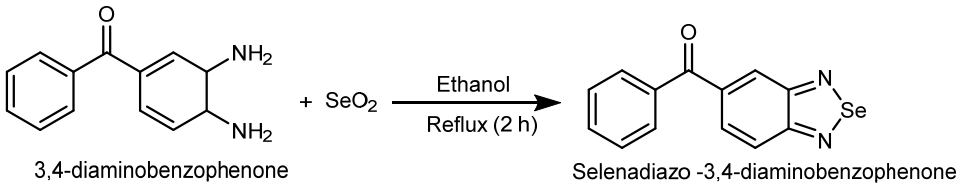

Scheme 1. Preparation of -3,4-selenadiazo benzophenone compound

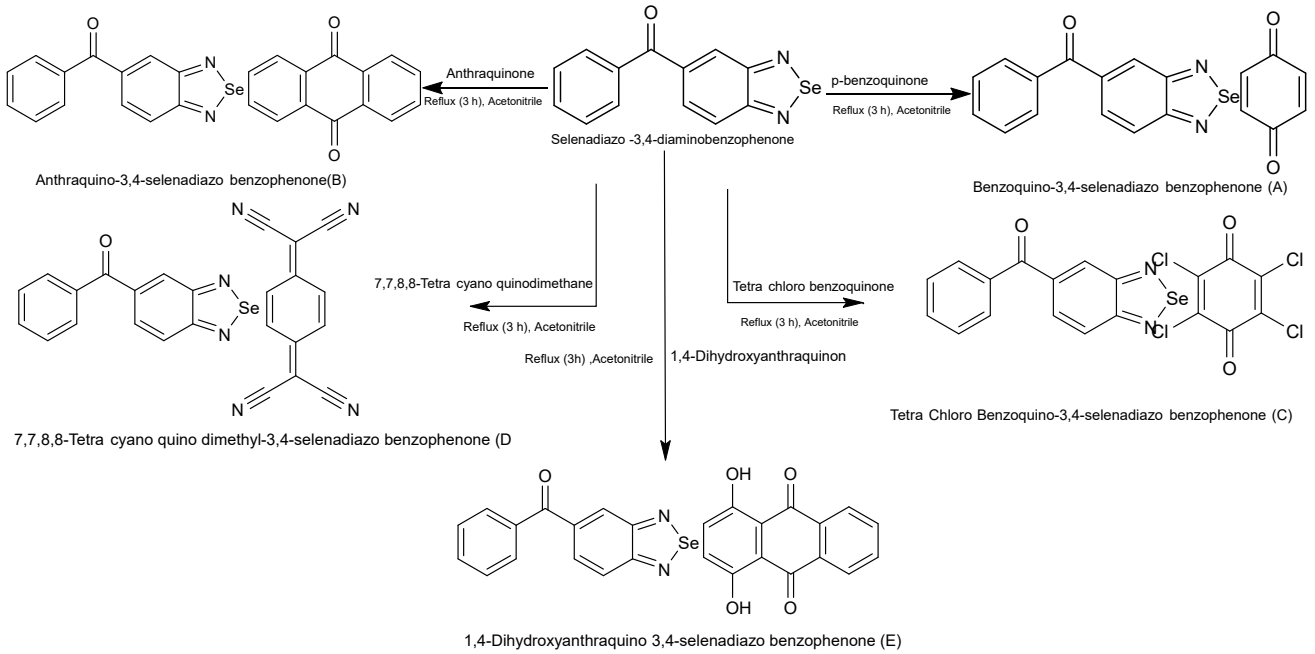

Scheme 2. Preparation of quino-3,4-selenadiazo benzophenone compounds A, B, C, D, E

to obtain a pure and shiny dark brown crystals precipitate formed with a yield of 85% and a melting point of 110 °C, as shown in Scheme 2. Rf value = 0.66 (7:3) (Ethyl acetate:*n*-hexane).

Preparation of 7,7,8,8-tetracyanoquinodimethyl-3,4-selenadiazo benzophenone (D)

3,4-Selenadiazo benzophenone (1.147 g, 4 mmol) was dissolved in 30 mL of acetonitrile and mixed with 0.816 g (4 mmol) of 7,7,8,8-tetracyanoquinodimethane dissolved in 30 mL of acetonitrile and heated using reflux in a water bath for 3 h. The solution was cooled and evaporated by a rotary evaporator and washed with small amounts of acetonitrile to obtain a pure and shiny dark yellow crystals precipitate formed with a yield of 82% and a melting point of 160 °C, as shown in Scheme 2. Rf value = 0.62 (7:3) (Ethyl acetate:*n*-hexane).

Preparation of 1,4-dihydroxyanthraquino 3,4-selenadiazo benzophenone (E)

3,4-Selenadiazo benzophenone (1.147 g, 4 mmol) was dissolved in 30 mL of acetonitrile and mixed with 0.960 g (4 mmol) of 1,4-Dihydroxyanthraquinon dissolved in 30 mL of acetonitrile and heated using reflux in a water bath for 3 h. The solution was cooled and evaporated by a rotary evaporator and washed with small amounts of acetonitrile to obtain a pure and shiny pink-yellow precipitate formed with a yield of 71% and a melting point of 170 °C, as shown in Scheme 2. Rf value = 0.86 (7:3) (Ethyl acetate:*n*-hexane).

■ RESULTS AND DISCUSSION

The present study involved the preparation of charge transfer complexes compounds derived from 3,4-selenadiazo benzophenone [19] (that was prepared in the first step) by reacting 3,4-selenadiazo benzophenone with different quinones in acetonitrile to obtain a series of charge transfer complexes (A–E). The UV-visible spectra were recorded from 200–750 nm. In DMSO as a solvent, there are two types of electronic transitions of n-π^* and π-π^* as provided in Fig. S1 [29-30] and Table 1. The n-π^* transitions experience a significant blue shift. The development of complexes and the deviating electron cloud around the selenium atom are responsible for this alteration. The electron donors and quinones decrease the transition of π-π^* and n-π^* conjugate effects in the group of the chromophore, and the energy required for the π-π^* and n-π^* transitions increase. As a result, the absorption band shifted toward shorter wavelengths.

Table 1. UV-Visible (λ_{max} nm) spectral data of selected compounds

Seq.	Compound	λ_{max} (C=C)	λ_{max} (C=O)	λ_{max} (C=N)	λ_{max} (C-Cl)	λ_{max} (C≡N)	λ_{max} (C-OH)
1	3,4-Selenadiazo benzophenone	225	273	355			
2	A	215	286	355			
3	B	220	285	365			
4	C	220	300	350	455		
5	D	235	275	387		450	
6	E	230	295	340			490

The IR spectra of all prepared compounds showed common elements in characteristic bands and specific regions in the fingerprint and other locations. The proposed structures of the synthesized compounds were verified using the IR spectrum [28,31] as provided in Table 2 as well as Fig. S2–S7. Table 2 showed all the expected peaks for 3,4-selenadiazo benzophenone and charge transfer complexes derivatives.

^{1}H-NMR spectra [28,31] showed all the expected peaks. The explanations for each spectrum are provided in the DMSO solvent of the compounds (A–E), as shown in Table 3 and Fig. S8–S13.

The 13C of the first compound (3,4-Selenadiazo benzophenone) was measured as shown in Fig. S14. ^{13}C-NMR (500 MHz, DMSO-d_6): Ar. $_{6}$C δ 126.6 (1C, s), Ar. $_{9}$C 127.1 (1C, s), Ar. $_{15}$C 127.8 (1C, s), Ar. $_{8}$C 127.9 (1C, s), Ar. ($_{14}$C, $_{16}$C) 128.4 (2C, s), Ar. ($_{13}$C, $_{17}$C) 129.0 (2C, s), Ar. $_{7}$C 129.3 (1C, s), Ar. $_{12}$C 137.2 (1C, s), Ar. ($_{3}$C, $_{4}$C) 160.4–160.6 (2C, 160.5 (s), 160.5 (s)), Ar. $_{10}$C 195.0 (1C, s).

Computational Analysis

All the charge-transfer complex compounds of 3,4-selenadiazobenzophenon under investigation were labeled as seen in Fig. S15. The method's accuracy in describing the compound's characteristics in the gas phase was evaluated. The Density functional theory (DFT) at B3LYP (hybrid functional), the available computational levels which combine Lee, Yang, and Parr's correlation with Becke's exchange, was used to study the electronic properties and geometric structures in all quantum calculations [32-33]. Using the basis set of 3–21G and the Gaussian 09W software, this method described every atom [29]. Using estimated DFT-based descriptors, the compounds' reactivity and stability were assessed using Eq. (1-4) [30,34].

$$\mu = \left(\frac{\delta E}{\delta N}\right)_{V(\vec{r}),T} \quad (1)$$

$$\eta = \frac{1}{2}\left(\frac{\delta^2 E}{\delta N^2}\right)_{V(\vec{r}),T} \quad (2)$$

Table 2. FTIR spectral data of selected compounds

Functional group	Compounds					
	3,4-Selenadiazo benzophenone	A	B	C	D	E
Ar. C–H	3061	3064	3070	3064	3051.49	3026.41
Ar. (C=O)	1649	1639	1678	1691.63	1639.55	1691.63
Ar. C=N	1579–1600	1575–1595	1577–1591	1570	1595.18	1591.33–1631.88
Ar. C=C	1490–1500	1433–1500	1450–1471	1489	1543	1454.38
Aliphatic C=C	-	-	-	-	1543	-
Ar. C-Se-N	3248.54	3257	3221	3231	3138	3200
Aliphatic C≡N	-	-	-	-	2222	-
Ar. OH	-	-	-	-	-	3500–3600
Ar. C-Cl	-	-	-	550–880	-	-

Table 3. ^{1}H-NMR spectral data of selected compounds

Seq.	Compounds	Structure of the compound	^{1}H-NMR (DMSO-d_6); TMS = 0 ppm
1	3,4-Selenadiazo benzophenone	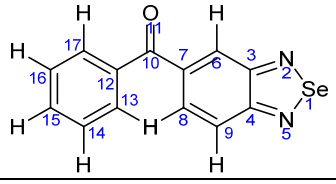	Ar. $_{14}$C-H, $_{16}$C-H (2H, t, δ 7.52); Ar. $_{15}$C-H, $_{17}$C-H (2H, m, δ 7.74); Ar. $_{13}$C-H, (1H, t, δ 7.88); Ar. $_{9}$C-H, (1H, d, δ 7.91); Ar. $_{8}$C-H, (1H, d, δ 8.01); Ar. $_{6}$C-H, (1H, s, δ 8.10).
2	(A)	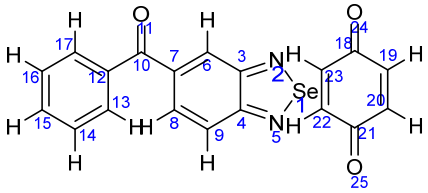	Ar. $_{15}$C-H, (1H, t, δ 7.75); Ar. $_{17}$C-H (1H, d, δ 7.87); Ar. $_{13}$C-H, $_{14}$C-H, $_{16}$C-H, $_{19}$C-H, $_{20}$C-H, $_{22}$C-H, $_{23}$C-H (7H, m, δ 7.56-7.64); Ar. $_{8}$C-H (1H, d, δ 7.9); Ar. $_{9}$C-H, (1H, d, δ 8.02); Ar. $_{6}$C-H, (1H, s, δ 8.10).
3	(B)	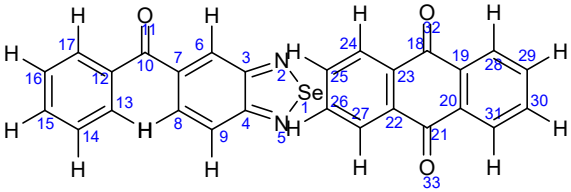	Ar. $_{14}$C-H, $_{16}$C-H(2H, m, δ 7.95); Ar. $_{15}$C-H, $_{17}$C-H, (2H, m, δ 7.89); Ar. $_{24}$C-H, $_{27}$C-H, $_{28}$C-H, $_{31}$C-H (4H, m, δ 8.23); Ar. $_{25}$C-H, $_{26}$C-H, $_{29}$C-H, $_{30}$C-H (4H, m δ 7.63); Ar. $_{13}$C-H, (1H, t, δ 7.88); Ar. $_{8}$C-H (1H, d, δ 8.02); Ar. $_{9}$C-H, (1H, d, δ 8.01); Ar. $_{6}$C-H, (1H, s, δ 8.10).
4	(C)	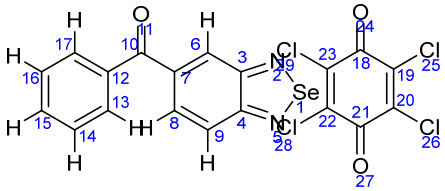	Ar. $_{14}$C-H, $_{16}$C-H (2H, m, δ 7.6); Ar. $_{15}$C-H, $_{17}$C-H (2H, m, δ 7.74); Ar. $_{13}$C-H, (1H, t, δ 7.86); Ar. $_{9}$C-H, (1H, d, δ 7.88); Ar. $_{8}$C-H, (1H, d, δ 8.00); Ar. $_{6}$C-H, (1H, s, δ 8.09).
5	(D)	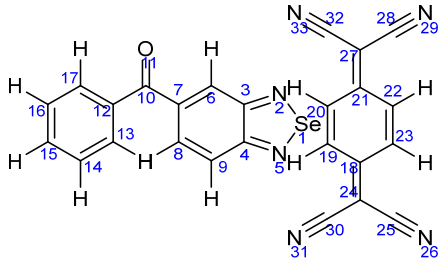	Ar. $_{15}$C-H, (1H, t, δ 7.62); Ar. $_{17}$C-H (1H, d, δ 7.75); Ar. $_{13}$C-H, $_{14}$C-H, $_{16}$C-H, (3H, m, δ 7.86); Ar. $_{8}$C-H (1H, d, δ 7.87); Ar. $_{9}$C-H, (1H, d, δ 8.00); Ar. $_{6}$C-H, (1H, s, δ 8.07).
6	(E)	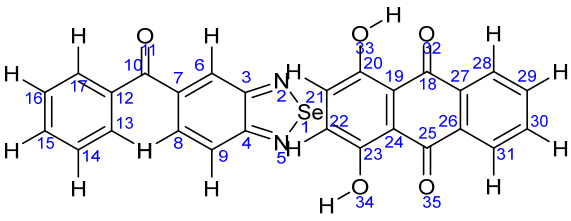	Ar. $_{14}$C-H, $_{16}$C-H(2H, m, δ 7.98); Ar. $_{15}$C-H, $_{17}$C-H, (2H, m, δ 7.89); Ar. $_{24}$C-H, $_{27}$C-H, $_{28}$C-H, $_{31}$C-H (4H, m, δ 7.44); Ar. $_{25}$C-H, $_{26}$C-H, $_{29}$C-H, $_{30}$C-H (4H, m, δ 7.41); Ar. $_{13}$C-H, (1H, t, δ 7.86); Ar. $_{8}$C-H (1H, d, δ 7.89); Ar. $_{9}$C-H, (1H, d, δ 8.02); Ar. $_{6}$C-H, (1H, s, δ 8.25). Ar. $_{33}$O-H, (2H, s, δ 12.65).

$$S = \frac{1}{2\eta} \quad (3)$$

$$\omega = \frac{\mu^2}{2\eta} \quad (4)$$

where μ, η, S, and ω are chemical potential, chemical hardness, chemical softness and electrophilicity, respectively., While E, N, and V($\vec{r}$) are the total electron energy, number of electrons and the external potential,

respectively. The above global quantities were calculated using two variations approaches; the first is a finite approximation difference, which is based on the variations in total electronic energies when an electron is added or removed after the neutral molecule. The second is Koopman's theorem, which is based on the variations in energies of HOMO and LUMO for molecules [30,34-35]. A finite difference approximation is used to the quantities of global, which can be given by Eq. (5-6).

$$\chi = \frac{(IP + EA)}{2} \quad (5)$$

$$\eta = \frac{(IP - EA)}{2} \quad (6)$$

Koopman's theory is given by Eq. (7-8):

$$\chi = \frac{(E_{HOMO} + E_{LUMO})}{2} \quad (7)$$

$$\eta = \frac{(E_{HOMO} - E_{LUMO})}{2} \quad (8)$$

A B3LYP functional in G09W and the standard 3-21G basis set for all charge-transfer complex compounds in the gaseous phase were used to obtain the equilibrium geometries. Compounds were thoroughly optimized at the DFT level of theory (see Fig. S16). The energy of the Highest Occupied Molecular Orbital (HOMO), and the Lowest Unoccupied Molecular Orbital (LUMO) is the electronic states, describing specific places where electrons with quantized energy exist, where the atomic orbitals and molecular orbitals combine linearly. The difference between LUMO and HOMO gives the energy band gap (Eg) as presented in Eq. (9) [36].

$$Eg = E_{LUMO} - E_{HOMO} \quad (9)$$

The property of the bandgap energy is fundamental in solids because it allows the material prediction, whether it is a semiconductor, insulator, or conductor. It is the difference in energy between the higher whole energy level and the lower virtual energy level [37] (see Fig. S16 and Table 4).

Electrophilicity and electronegativity

The ability of a molecule to take up electrons is measured by chemical electrophilicity, which is based on the chemical hardness and chemical potential, where hardness is defined as resistance to deformation and change. Electronegativity, on the other hand, is a measurement of an atom's ability to attract an electron density (or shared pair of electrons) towards itself. Eq. (10) and (11) [32,38] can be used to compute electronegativity (χ) and electrophilicity (w) and the result can be seen in Table 5.

$$\chi = \frac{(E_{HOMO} + E_{LUMO})}{2} \quad (10)$$

$$w = \frac{\chi^2}{2\eta} \quad (11)$$

Table 4. The electronic states of the charge-transfer complex compounds

Compound	HOMO (eV)	LUMO (eV)	Eg (eV)
3,4-Selenadiazo benzophenone	-6.4272741	-2.8848	3.54247
A	-5.2267689	-3.23962	1.987146
B	-4.8909975	-2.7629	2.128094
C	-5.9358615	-4.27143	1.664436
D	-5.9418477	-0.49332	5.44853
E	-4.9367103	-3.01922	1.917489

Table 5. Electronegativity and electrophilicity of the charge-transfer complex compounds

Compound	Electronegativity (eV) (X)	Electrophilicity (eV) (w)
3,4-Selenadiazo benzophenone	-4.65604	-6.11966
A	-4.2332	-9.01794
B	-3.82695	-6.882
C	-5.10364	-15.6492
D	-3.21758	-1.90011
E	-3.97797	-8.25258

Electron affinity and ionization potential

The energy produced when an atom gains an electron is known as electron affinity. The energy is necessary to expel an electron from a negatively charged ion. The ionization potential measures the force of the bonding between the electron and the atom. It is equivalent to the energy needed to remove one electron from a neutral atom in the gas phase. As seen in Table 6, this is Koopman's idea [32].

$$IP = -E_{HOMO} \quad (12)$$

$$EA = -E_{LUMO} \quad (13)$$

Eq. (12) represents the ionization energy (IP), while Eq. (13) represents the energy of electronic affinity (EA).

Acid-base hardness softness (HSAB principle)

This principle explains how atoms or molecules behave when used as acids and bases in chemistry. First, it must be demonstrated that whereas soft and hard bases stand for donors, soft and hard acids represent acceptors. Eq. (14) and (15) [39-41] can be used to express hardness Eq. (14) and softness Eq. (15).

$$\eta = \frac{(IP - EA)}{2} \quad (14)$$

$$\delta = \frac{1}{2\eta} \quad (15)$$

Chemical hardness and softness are denoted by the symbols (η) and (σ), respectively, according to Table 6.

In the present study, a comparison of the HOMO energies is presented in Table 4 to find out that the HOMO energy of D compound is greater than that of A, C, and E compounds, and the lowest in HOMO energy was B compound, and the arrangement of the energy average [42] [in LUMO energy is as follows: C > A > E > B > D. As a result, the energy gap is greatest at the D compound and lowest at the C compound [42].

In Table 5, the electronegativity of C was larger than the electronegativity of A, B, D, and E. The C compound was the largest electrophilic molecule, whereas D has the least electrophilicity among all prepared compounds [43-44].

According to Table 6, the behavior of organoselenium compounds can be classified as donors or acceptors through a comparison between A, B, C, D, and E. The hardness of D is greater than the hardness of A, B, C and E; hence D will behave as a hard base. The softness of C was greater than that of A, B, D and E, indicating that C will behave as a soft base [44-45].

■ CONCLUSION

The current work describes straightforward and practical ways to synthesize various novel charge-transfer complex compounds. Compounds A, B, C, D, and E were synthesized with a 71–90% yield. The current study's investigation of the UV-visible Spectrophotometer, FTIR, and ^{1}H-NMR agrees with other studies in these fields. They confirm the suggested structures' accuracy for all the synthesized compounds. Regarding the theoretical investigation, it can be said that the B3LYP functional is an appropriate and practical approach, and the density functional theory employed in this investigation is a powerful method to investigate these structures' electronic characteristics. The experimental data agreed with the geometrical properties of 3-21G (d, p). This work employs the DFT approach to investigate the electronic characteristics of

Table 6. The charge-transfer complex compounds have ionization potential, electron affinity, hardness, and softness

Compound	Ionization potential (eV) (I.P)	Electron affinity (eV) (E.A)	Hardness (η)	Softness (δ)
3,4-Selenadiazo benzophenone	6.4272741	2.8848042	-1.77123	-0.28229
A	5.2267689	3.2396226	-0.99357	-0.50323
B	4.8909975	2.7629034	-1.06405	-0.4699
C	5.9358615	4.2714258	-0.83222	-0.6008
D	5.9418477	0.4933173	-2.72427	-0.18354
E	4.9367103	3.0192216	-0.95874	-0.52152

charge-transfer complex compounds and geometry optimization by using the available B3LYP. The total energies donor-acceptor system and geometric structures demonstrate this structure's stability. Additionally, the donor-acceptor system has higher reactivity than other systems and larger average polarizability when compared to the donor and acceptor. The findings of this study enable us to choose the kind of bridge that will interact with the donor and acceptor to determine the physical characteristics of the donor-bridge-acceptor.

■ REFERENCES

[1] Wirth, T., 2012, *Organoselenium Chemistry: Synthesis and Reactions*, Wiley-VCH, Weinheim, Germany.

[2] Asmus, S., Nyulászi, L., and Regitz, M., 2001, Formation of selenaphosphole isomers from 1,2,4-selenadiphosphole by cycloaddition reaction. A synthetic and *ab initio* quantum chemical study, *J. Chem. Soc., Perkin Trans.*, 2 (10), 1968–1972.

[3] Potts, K.T., Cody, R.D., and Dennis, R.J., 1981, Nonclassical heteropentalenes containing the selenodiazole, thiatriazole and selenotriazole ring systems, *J. Org. Chem.*, 46 (20), 4065–4068.

[4] Rakitin, O.A., 2020, Fused 1,2,5-thia- and 1,2,5-selenadiazoles: Synthesis and application in materials chemistry, *Tetrahedron Lett.*, 61 (34), 152230.

[5] Hassan, A.F., Radhy, H.A., and Essa, A.H., 2009, Synthesis and study of charge-transfer complexes for 5,6-dimethyl-2,1,3-benzoselenadiazole, *J. Sci. Res.*, 1 (3), 569–575.

[6] Konstantinova, L.S., Knyazeva, E.A., and Rakitin, O.A., 2014, Recent developments in the synthesis and applications of 1,2,5-thia-and selenadiazoles. A review, *Org. Prep. Proced. Int.*, 46 (6), 475–544.

[7] Xia, Z.L., Xu-Xu, Q.F., Zheng, C., and You, S.L., 2020, Chiral phosphoric acid-catalyzed asymmetric dearomatization reactions, *Chem. Soc. Rev.*, 49 (1), 286–300.

[8] Semenov, N.A., Gorbunov, D.E., Shakhova, M.V., Salnikov, G.E., Bagryanskaya, I.Y., Korolev, V.V., Beckmann, J., Gritsan, N.P., and Zibarev, A.V., 2018, Donor–acceptor complexes between 1,2,5-chalcogenadiazoles (Te, Se, S) and the pseudohalides CN^- and XCN^- (X= O, S, Se, Te), *Chem. - Eur. J.*, 24 (49), 12983–12991.

[9] Ren, L., Xian, X., Yan, K., Fu, L., Liu, Y., Chen, S., and Liu, Z., 2010, A general electrochemical strategy for synthesizing charge-transfer complex micro/nanowires, *Adv. Funct. Mater.*, 20 (8), 1209–1223.

[10] Ratera, I., and Veciana, J., 2012, Playing with organic radicals as building blocks for functional molecular materials, *Chem. Soc. Rev.*, 41 (1), 303–349.

[11] Mostafa, A., El-Ghossein, N., Cieslinski, G.B., and Bazzi, H.S., 2013, UV–Vis, IR spectra and thermal studies of charge transfer complexes formed in the reaction of 4-benzylpiperidine with σ- and π-electron acceptors, *J. Mol. Struct.*, 1054-1055, 199–208.

[12] Yakuphanoglu, F., and Arslan, M., 2004, The fundamental absorption edge and optical constants of some charge transfer compounds, *Opt. Mater.*, 27 (1), 29–37.

[13] Saito, G., and Yoshida, Y., 2007, Development of conductive organic molecular assemblies: Organic metals, superconductors, and exotic functional materials, *Bull. Chem. Soc. Jpn.*, 80 (1), 1.

[14] Bai, H., Wang, Y., Cheng, P., Li, Y., Zhu, D., and Zhan, X., 2014, Acceptor–donor–acceptor small molecules based on indacenodithiophene for efficient organic solar cells, *ACS Appl. Mater. Interfaces*, 6 (11), 8426–8433.

[15] Ng, T.W., Lo, M.F., Fung, M.K., Zhang, W.J., and Lee, C.S., 2014, Charge-transfer complexes and their role in exciplex emission and near-infrared photovoltaics, *Adv. Mater.*, 26 (31), 5569–5574.

[16] Heiska, J., Nisula, M., and Karppinen, M., 2019, Organic electrode materials with solid-state battery technology, *J. Mater. Chem. A*, 7 (32), 18735–18758.

[17] Zhang, J., Xu, W., Sheng, P., Zhao, G., and Zhu, D., 2017, Organic donor–acceptor complexes as novel organic semiconductors, *Acc. Chem. Res.*, 50 (7), 1654–1662.

[18] El-Habeeb, A.A., Al-Saif, F.A., and Refat, M.S., 2013, Charge transfer complex of some nervous and brain drugs – Part 1: Synthesis, spectroscopic,

analytical and biological studies on the reaction between haloperidol antipsychotic drugs with π-acceptors, *J. Mol. Struct.*, 1034, 1–18.

[19] Zulkarnain, Z., Khan, I.M., Ahmad, A., Miyan, L., Ahmad, M., and Azizc, N., 2017, Synthesis of charge transfer complex of chloranilic acid as acceptor with *p*-nitroaniline as donor: Crystallographic, UV–visible spectrophotometric and antimicrobial studies, *J. Mol. Struct.*, 1141, 687–697.

[20] Gaballa, A.S., and Amin, A.S., 2015, Preparation, spectroscopic and antibacterial studies on charge-transfer complexes of 2-hydroxypyridine with picric acid and 7,7′,8,8′-tetracyano-*p*-quinodimethane, *Spectrochim. Acta, Part A*, 145, 302–312.

[21] Duymus, H., Arslan, M., Kucukislamoglu, M., and Zengin, M., 2006, Charge transfer complex studies between some non-steroidal anti-inflammatory drugs and π-electron acceptors, *Spectrochim. Acta, Part A*, 65 (5), 1120–1124.

[22] Semenov, N.A., Lonchakov, A.V., Gritsan, N.P., and Zibarev, A.V., 2015, Donor-acceptor coordination of anions by chalcogen atoms of 1,2,5-chalcogenadiazoles, *Russ. Chem. Bull.*, 64 (3), 499–510.

[23] Alfuth, J., Zadykowicz, B., Sikorski, A., Połoński, T., Eichstaedt, K., and Olszewska, T., 2020, Effect of aromatic system expansion on crystal structures of 1,2,5-thia-and 1,2,5-selenadiazoles and their quaternary salts: synthesis, structure, and spectroscopic properties, *Materials*, 13 (21), 4908.

[24] Hasegawa, T., 2017, *Quantitative Infrared Spectroscopy for Understanding of a Condensed Matter*, Springer, Tokyo.

[25] Chulanova, E.A., Semenov, N.A., Pushkarevsky, N.A., Gritsan, N.P., and Zibarev, A.V., 2018, Charge-transfer chemistry of chalcogen–nitrogen π-heterocycles, *Mendeleev Commun.*, 28 (5), 453–460.

[26] Zam, W., Alshahneh, M., and Hasan, A., 2019, Methods of spectroscopy for selenium determination: A review, *Res. J. Pharm. Technol.*, 12 (12), 6149–6152.

[27] Shi, P., Wang, J., Gan, Z., Zhang, J., Zeng, R., and Zhao, Y., 2019, A practical copper-catalyzed approach to β-lactams *via* radical carboamination of alkenyl carbonyl compounds, *Chem. Commun.*, 55 (71), 10523–10526.

[28] Silverstein, R.M., Webster, F.X., Kiemle, D.J., and Bryce, D.L., 2015, *Spectrometric Identification of Organic Compounds*, Wiley, Hoboken, NJ.

[29] Sadlej, J., Dobrowolski, J.C., and Rode, J.E., 2010, VCD spectroscopy as a novel probe for chirality transfer in molecular interactions, *Chem. Soc. Rev.*, 39 (5), 1478–1488.

[30] Lee, C., Yang, W., and Parr, R.G., 1988, Development of the Colle-Salvetti correlation-energy formula into a functional of the electron density, *Phys. Rev. B*, 37 (2), 785.

[31] Asadi, N., Ramezanzadeh, M., Bahlakeh, G., and Ramezanzadeh, B., 2020, Theoretical MD/DFT computer explorations and surface-electrochemical investigations of the zinc/iron metal cations interactions with highly active molecules from *Lemon balm* extract toward the steel corrosion retardation in saline solution, *J. Mol. Liq.*, 310, 113220.

[32] McClain, J., Sun, Q., Chan, G.K.L., and Berkelbach, T.C., 2017, Gaussian-based coupled-cluster theory for the ground-state and band structure of solids, *J. Chem. Theory Comput.*, 13 (3), 1209–1218.

[33] Ajeel, F.N., Khudhair, A.M., and Mohammed, A.A., 2015, Density functional theory investigation of the physical properties of dicyano pyridazine molecules, *Int. J. Sci. Res*, 4 (1), 2334–2339.

[34] Ajeel, F.N., 2017, Analytical insight into the effect of electric field on molecular properties of homonuclear diatomic molecules, *Curr. Smart Mater.*, 2 (2), 153–161.

[35] Jabbar, M.L., 2018, Theoretical study for the interactions of Coronene-Y interactions by using density functional theory with hybrid function, *Univ. Thi-Qar J.*, 13 (3), 28–41.

[36] Abd El-Lateef, H.M., Shaaban, S., Khalaf, M.M., Toghan, A., and Shalabi, K., 2021, Synthesis, experimental, and computational studies of water soluble anthranilic organoselenium compounds as safe corrosion inhibitors for J55 pipeline steel in acidic oilfield formation water, *Colloids Surf., A*, 625, 126894.

[37] Alparone, A., 2012, Structural, energetic and response electric properties of cyclic selenium clusters: An ab initio and density functional theory study, *Theor. Chem. Acc.*, 131 (6), 1239.

[38] Pereira, F., Xiao, K., Latino, D.A.R.S., Wu, C., Zhang, Q., and Aires-de-Sousa, J., 2017, Machine learning methods to predict density functional theory B3LYP energies of HOMO and LUMO orbitals, *J. Chem. Inf. Model.*, 57 (1), 11–21.

[39] Alwan, A.S., Ajeel, S.K., and Jabbar, M.L., 2019, Theoretical study for Coronene and Coronene-Al, B, C, Ga, In and Coronene-O interactions by using density functional theory, *Univ. Thi-Qar J.*, 14 (4). 1–14.

[40] Hanoon, F.H., Jabbar, M.L., and Alwan, A.S., 2017, Effect of thickness on the fractal optical modulator for MgF_2, LiF, Al_2O_3 materials by testing modulation transfer function (MTF), *J. Educ. Pure Sci.*, 7 (4), 168–182.

[41] Panhans, M., Hutsch, S., Benduhn, J., Schellhammer, K.S., Nikolis, V.C., Vangerven, T., Vandewal, K., and Ortmann, F., 2020, Molecular vibrations reduce the maximum achievable photovoltage in organic solar cells, *Nat. Commun.*, 11 (1), 1488.

[42] Jabbar, M.L., and Kadhim, K.J., 2021, Electronic properties of doped graphene nanoribbon and the electron distribution contours: A DFT study, *Russ. J. Phys. Chem. B*, 15 (1), 46–52.

[43] Hameed, A.J., Ibrahim, M., and ElHaes, H., 2007, Computational notes on structural, electronic and QSAR properties of [C60]fulleropyrrolidine-1-carbodithioic acid 2; 3 and 4-substituted-benzyl esters, *J. Mol. Struct.: THEOCHEM*, 809 (1-3), 131–136.

[44] Sani, M.J., 2021, Spin-orbit coupling effect on the electrophilicity index, chemical potential, hardness and softness of neutral gold clusters: A relativistic ab-initio study, *HighTech Innovation J.*, 2 (1), 38–50.

[45] Kim, H., and Choi, H.J., 2021, Thickness dependence of work function, ionization energy, and electron affinity of Mo and W dichalcogenides from DFT and GW calculations, *Phys. Rev. B*, 103 (8), 085404.

Supplementary Data

This supplementary data is a part of a paper entitled "Synthesis, Characterization, and Theoretical Study of Novel Charge-Transfer Complexes Derived from 3,4-Selenadiazobenzophenone".

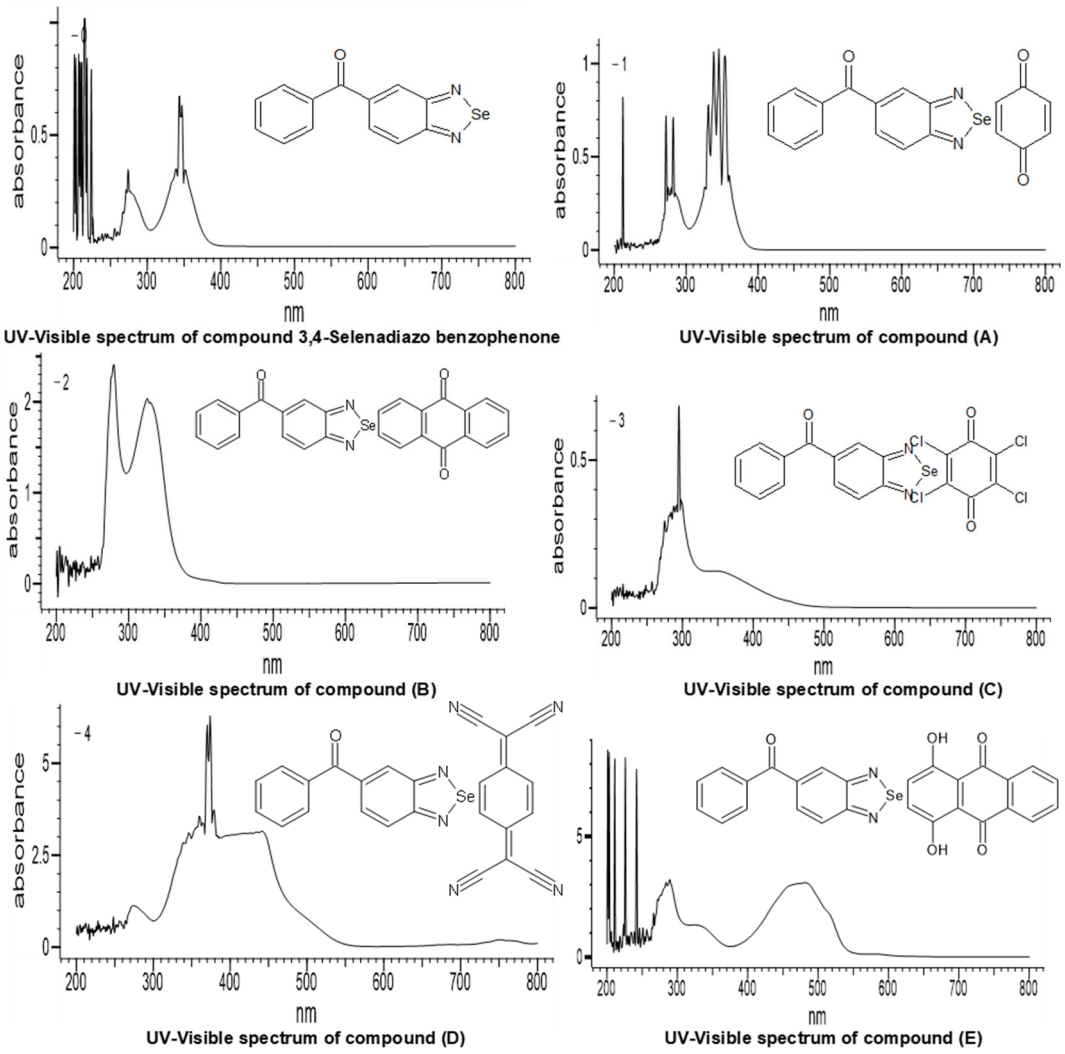

Fig S1. UV-Visible spectrum of compounds 3,4-Selenadiazo benzophenone, A, B, C, D, and E

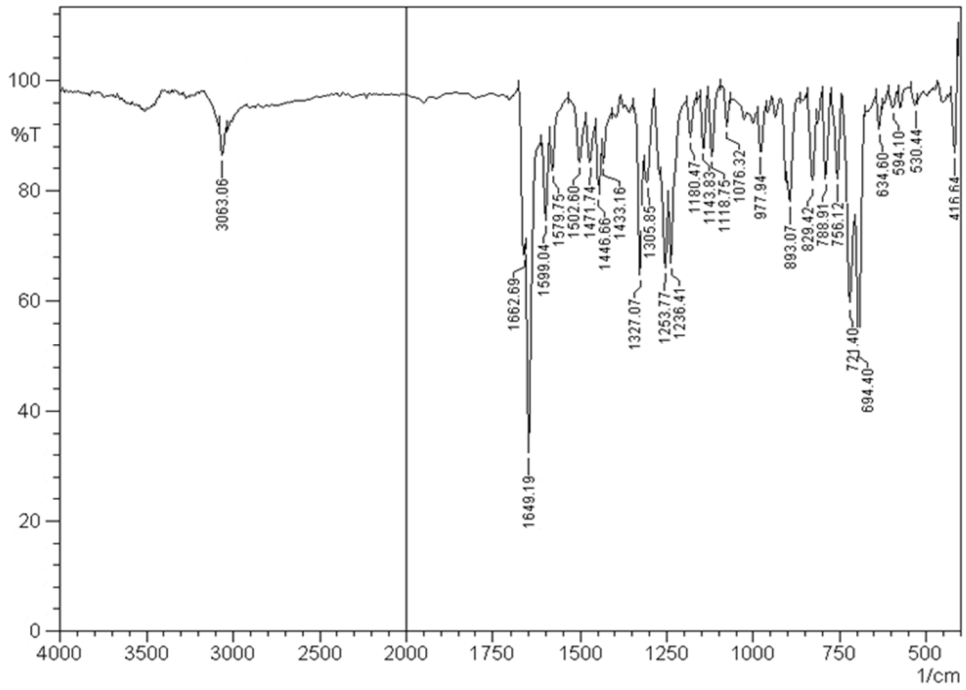

Fig S2. FTIR spectrum of 3,4-selenadiazo benzophenone

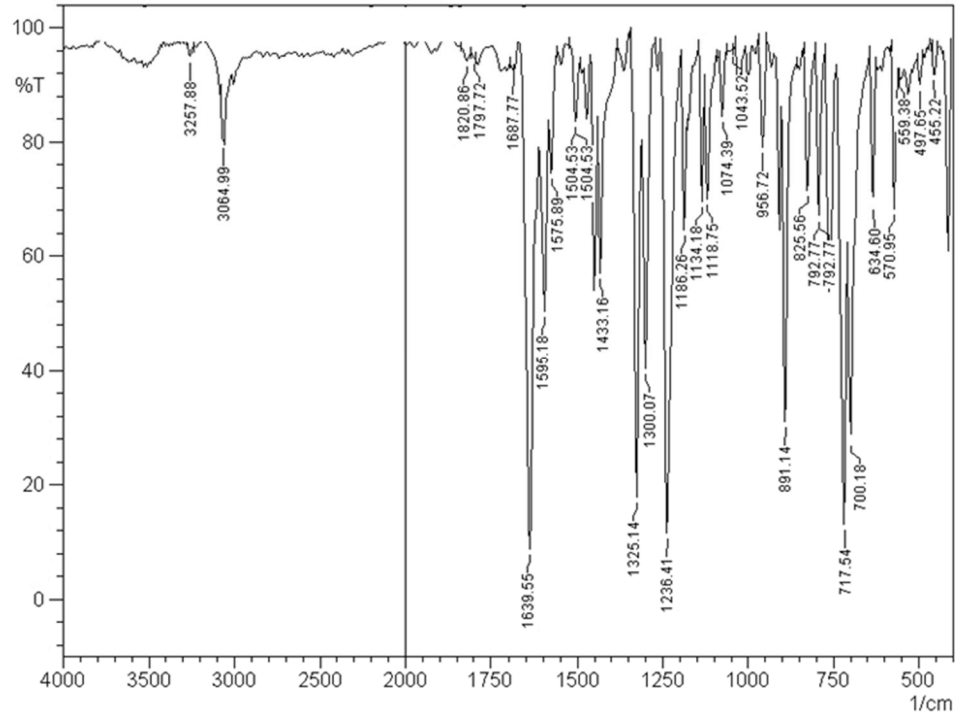

Fig S3. FTIR of compound A

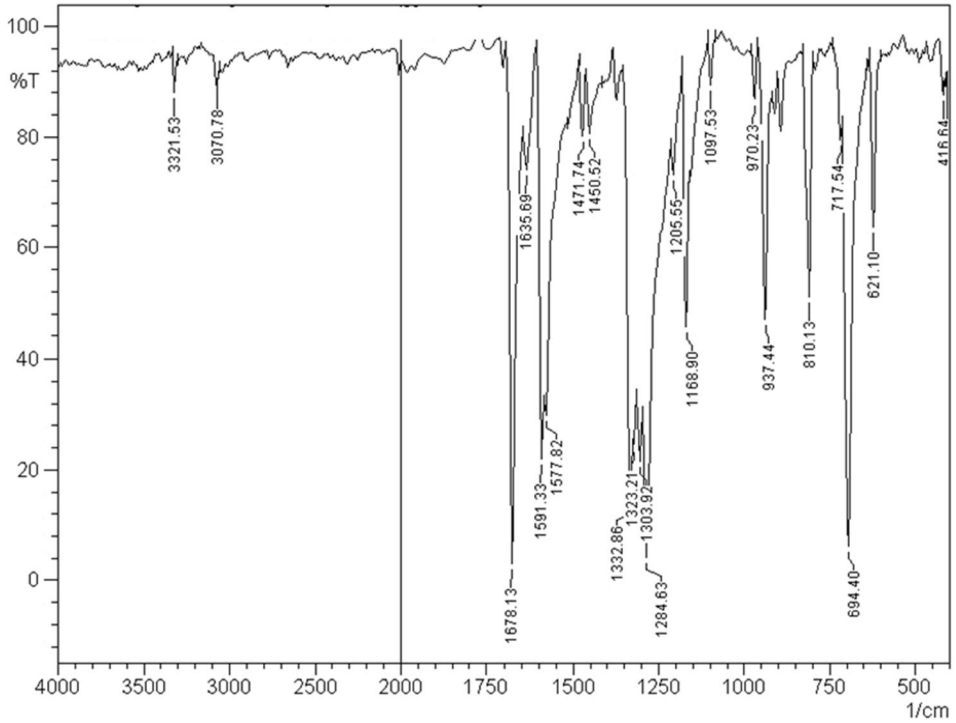

Fig S4. FTIR spectrum of compound B

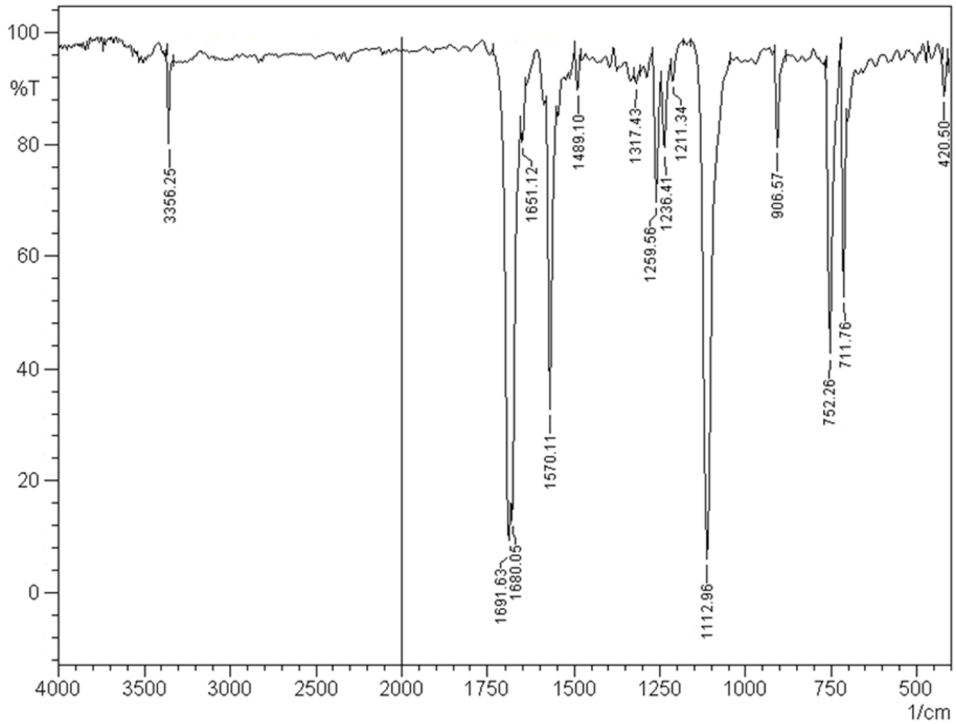

Fig S5. FTIR spectrum of compound (C)

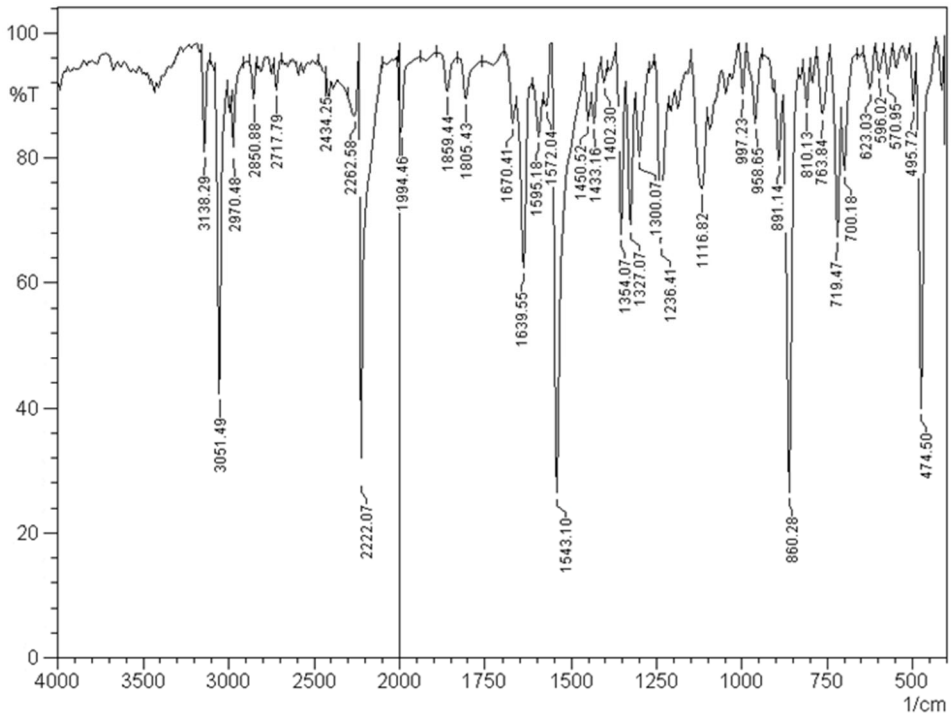

Fig S6. FTIR spectrum of compound D

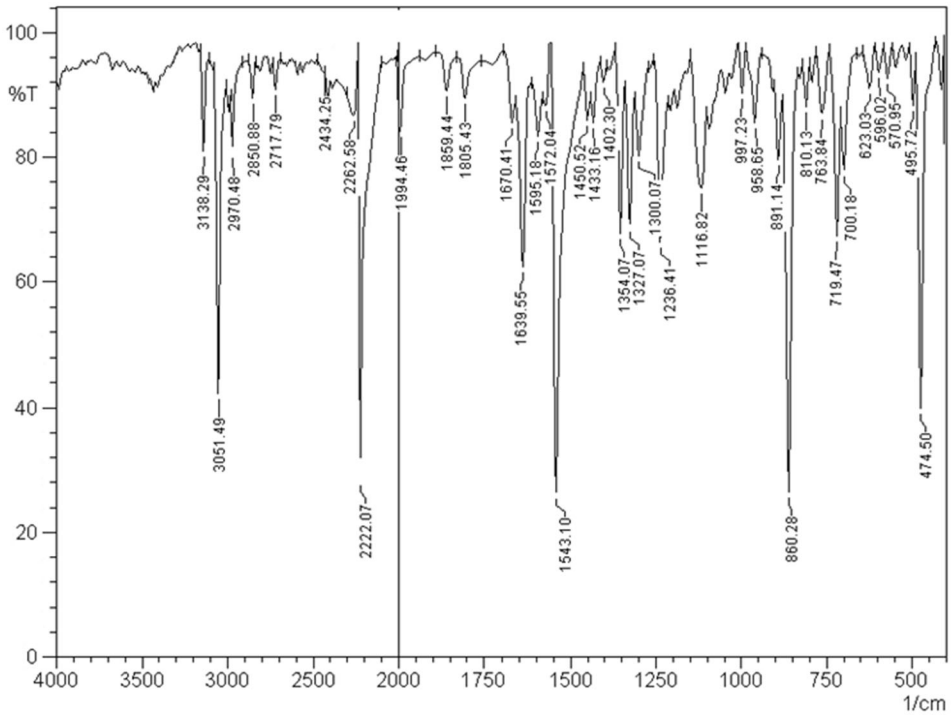

Fig S7. FTIR spectrum of compound E

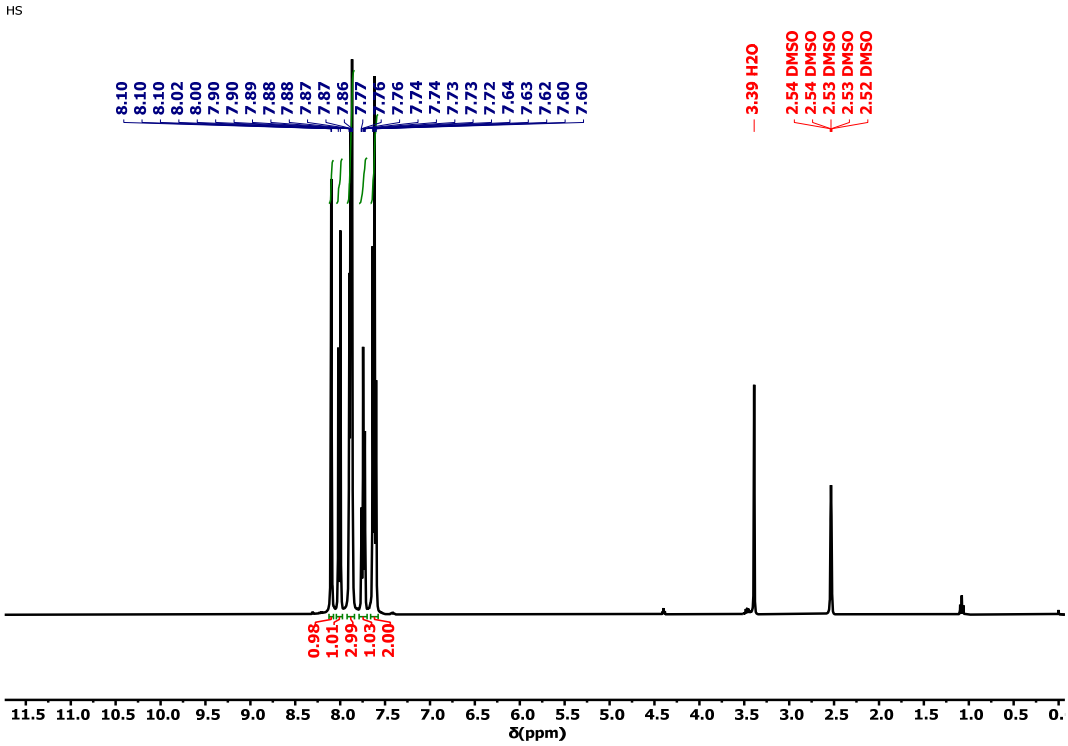

Fig S8. [1]H-NMR spectrum of compound 3,4-selenadiazo benzophenone

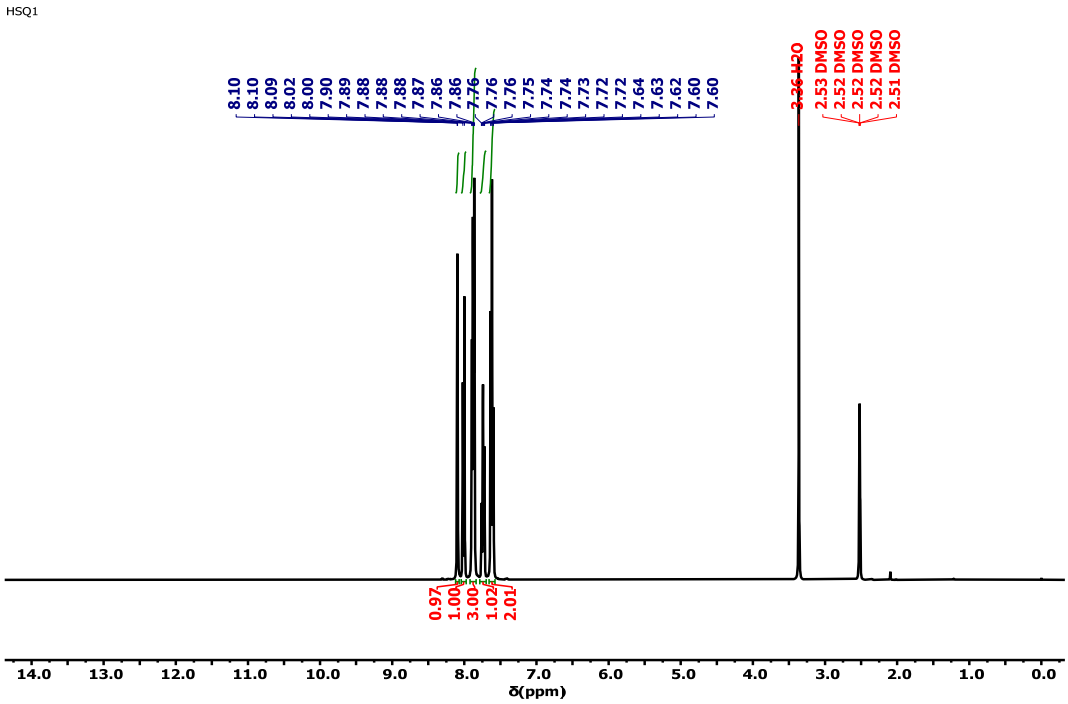

Fig S9. [1]H-NMR spectrum of compound A

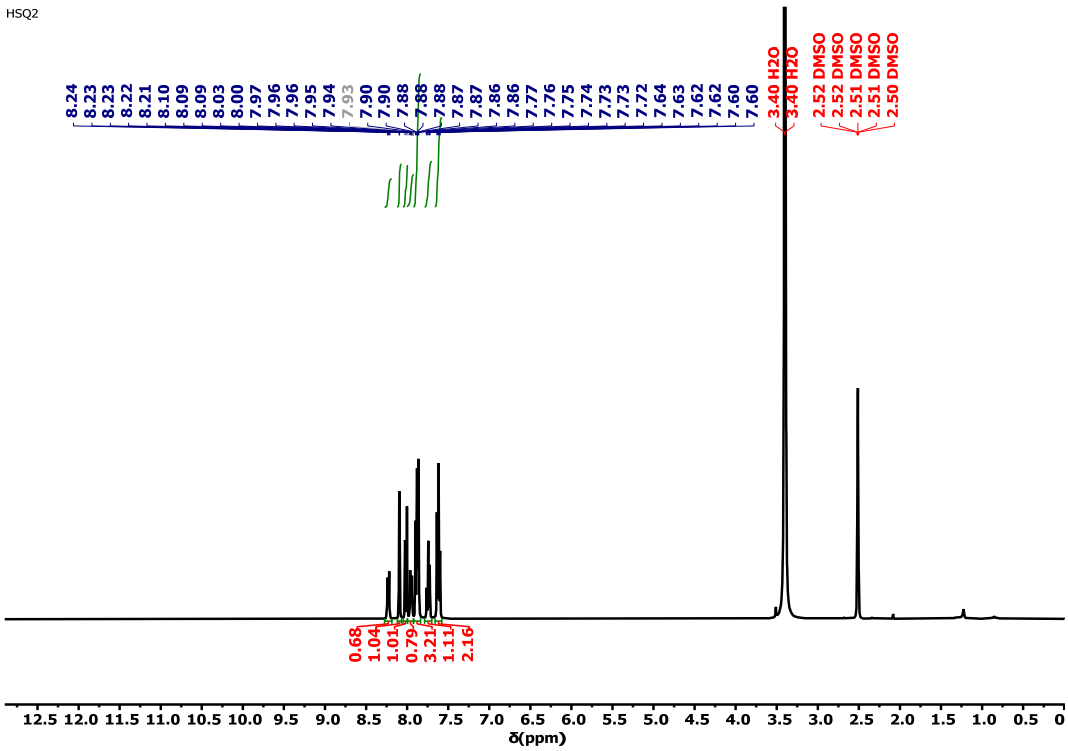

Fig S10. ^{1}H-NMR spectrum of compound B

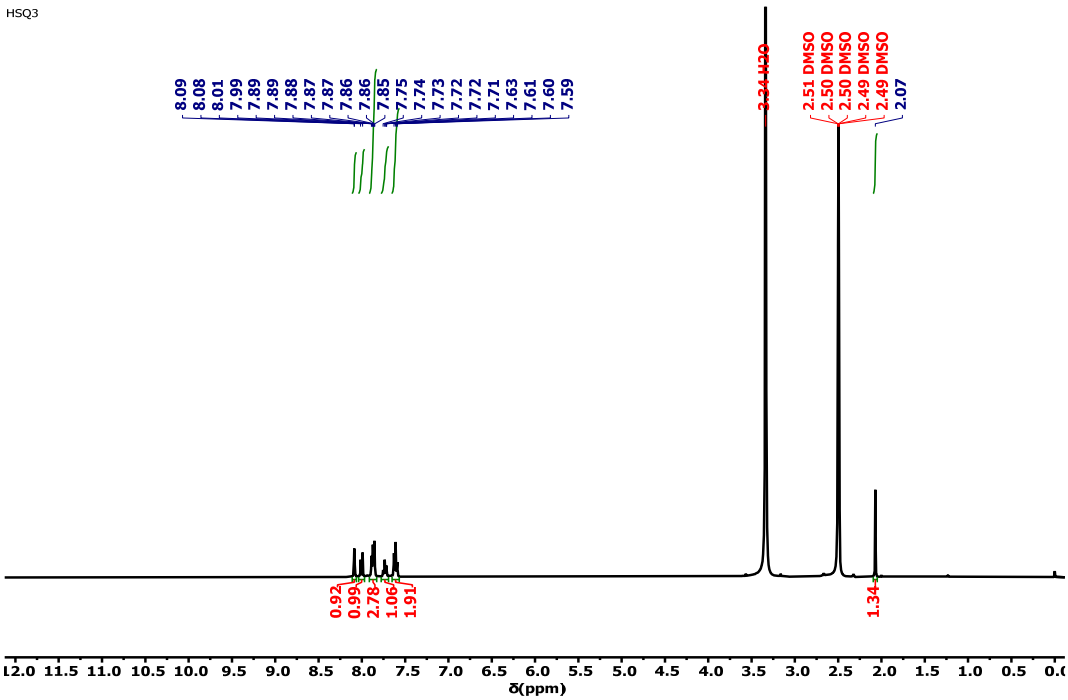

Fig S11. ^{1}H-NMR spectrum of compound C

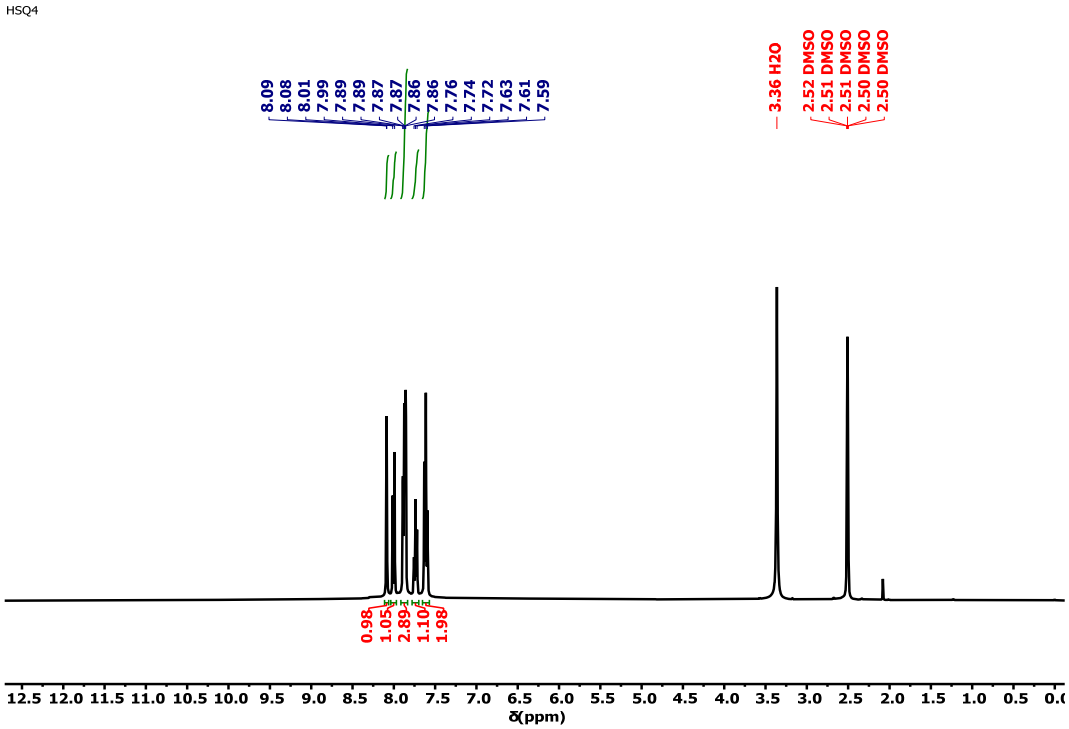

Fig S12. [1]H-NMR spectrum of compound D

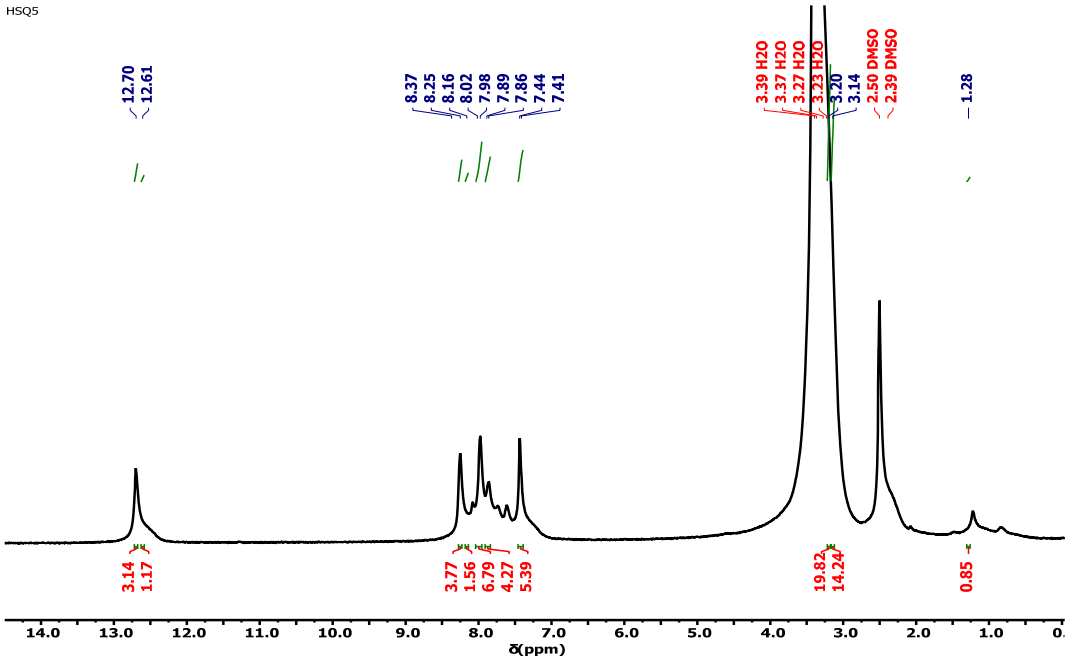

Fig S13.[1]H-NMR spectrum of compound E

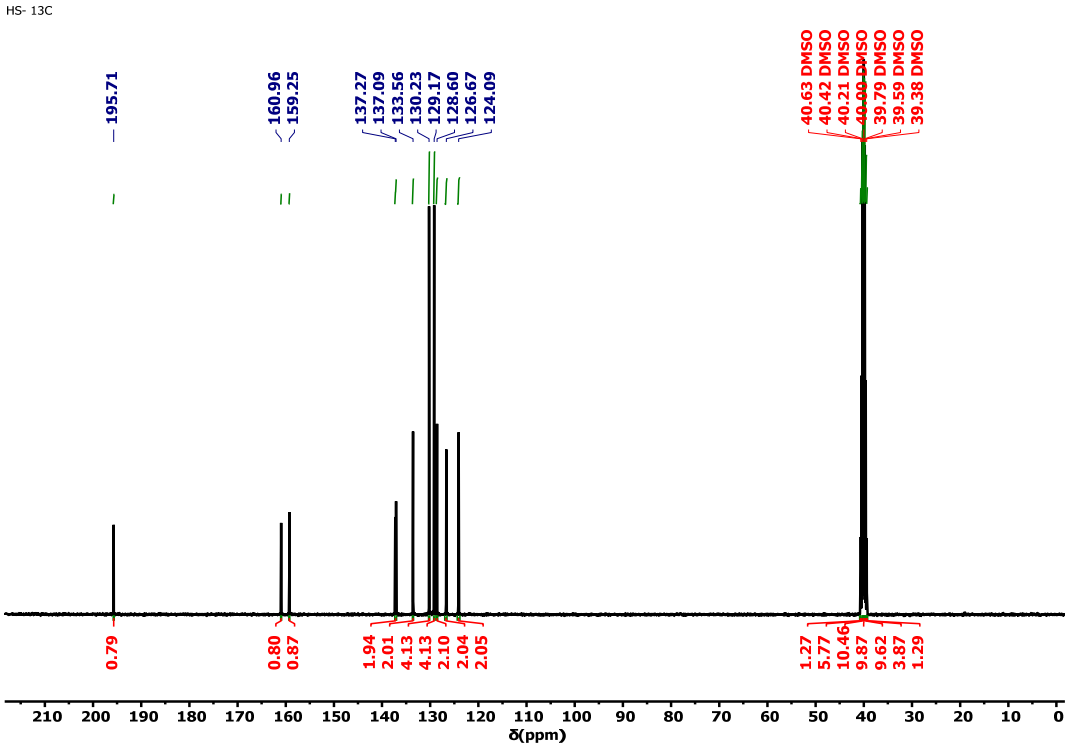

Fig S14. ^{13}C NMR spectrum of compound 3,4-selenadiazo benzophenone

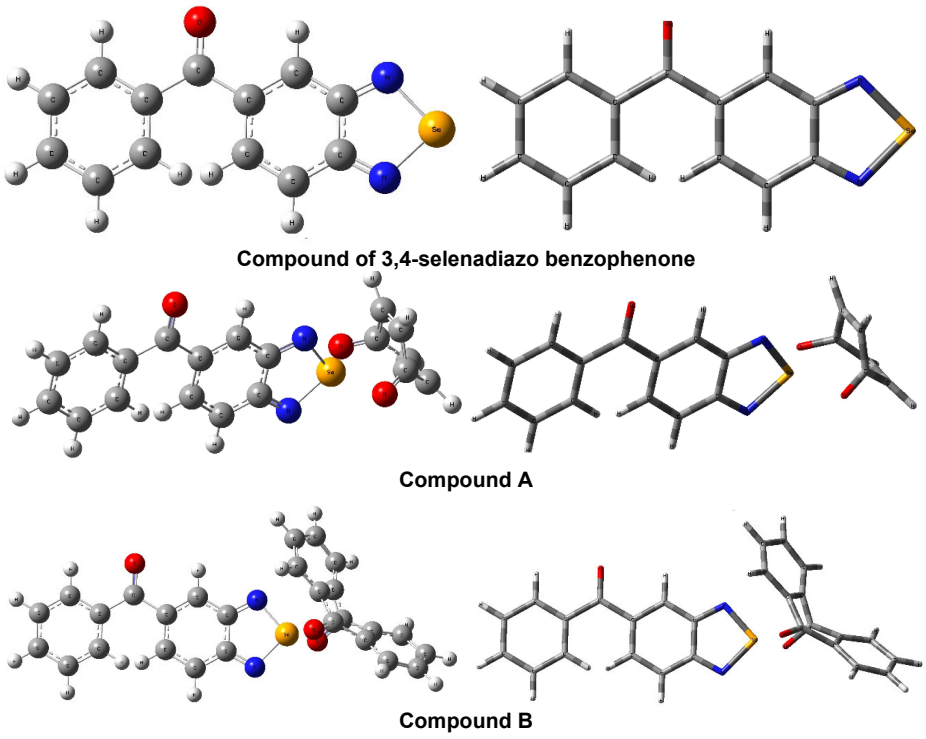

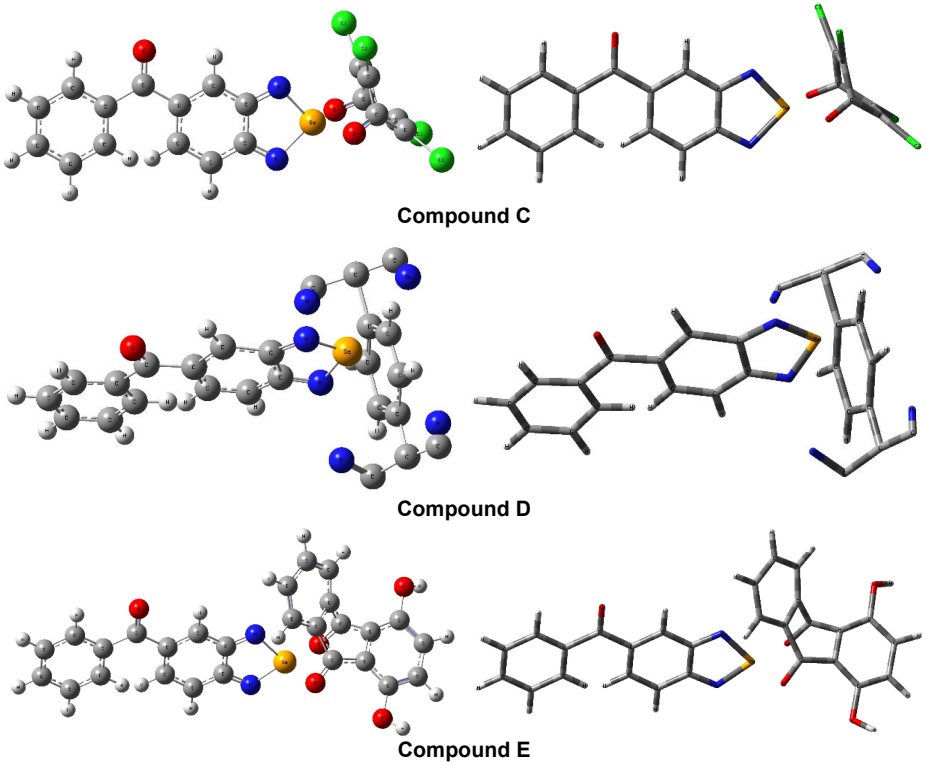

Fig S15. Molecular structure ball and tube model of compounds 3,4-selenadiazo benzophenone, A, B, C, D, and E

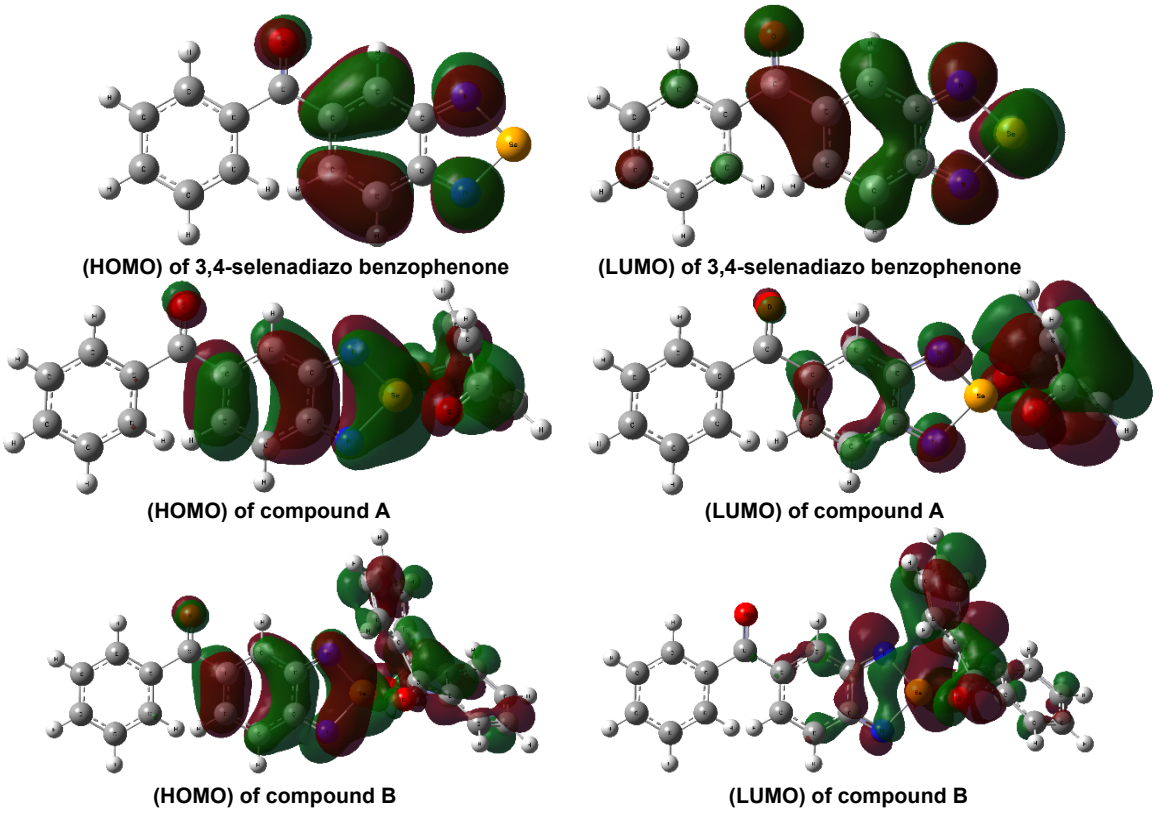

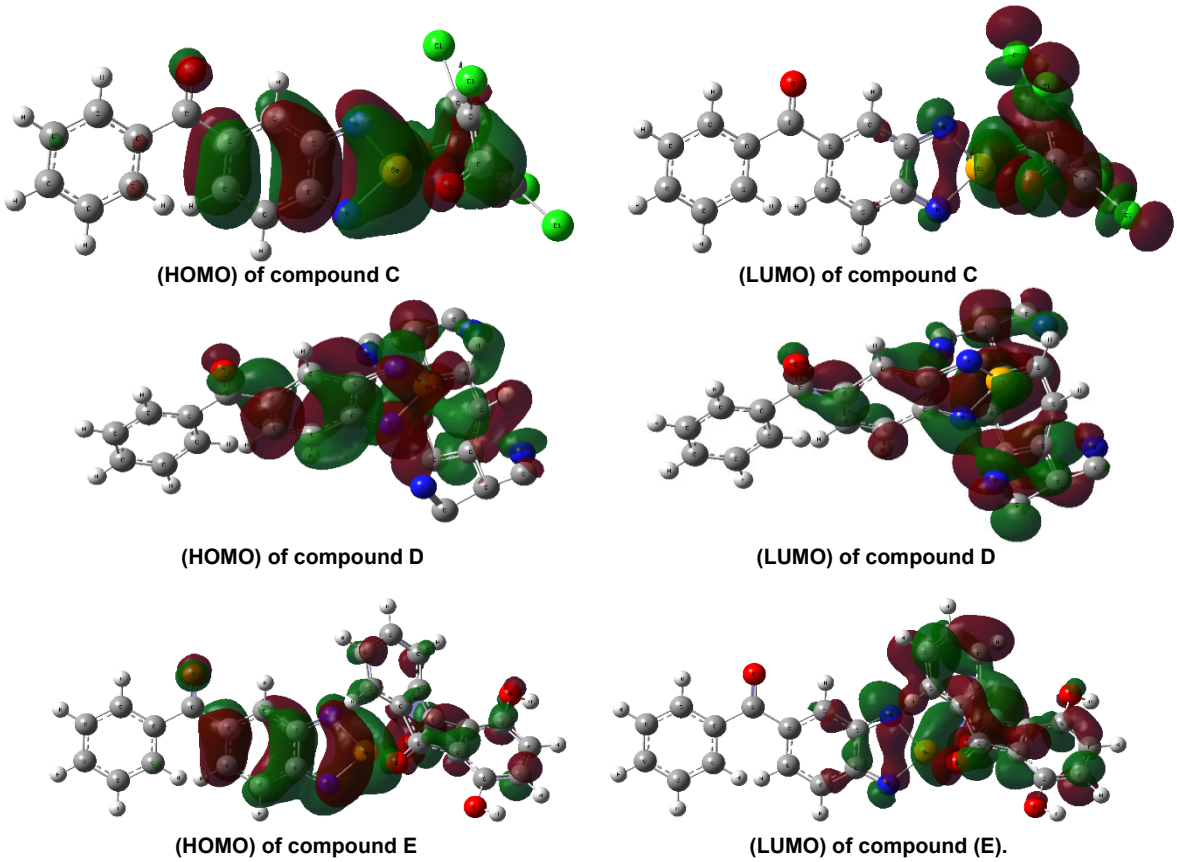

Fig S16. Molecular orbital HOMO and LUMO of compounds 3,4-selenadiazo benzophenone, A, B, C, D, and E